IJCRT.ORG ISSN : 2320-2882

INTERNATIONAL JOURNAL OF CREATIVE RESEARCH THOUGHTS (IJCRT)

An International Open Access, Peer-reviewed, Refereed Journal

ANFIS-CONTROLLED BIDIRECTIONAL DC-DC BUCK-BOOST CONVERTER WITH VOLTAGE SOURCE INVERTER FOR BLDC MOTOR DRIVE AND BATTERY MANAGEMENT: DESIGN, SIMULATION, AND PERFORMANCE ANALYSIS USING MATLAB/SIMULINK

[1]Punya K T, [2]Dr. G.S Sheshadri

[1]PG Scholar, Department of Electrical & Electronics, Sri Siddhartha Institute of Technology, SSAHE, Tumkur, Karnataka [2], Associate Professor, Department of Electrical & Electronics, Sri Siddhartha Institute of Technology, SSAHE, Tumkur, Karnataka, India

Doi : https://doi.org/10.56975/ijcrt.v14i7.309928

Abstract: This paper presents the design, modeling, and simulation of an Adaptive Neuro-Fuzzy Inference System (ANFIS)-controlled bidirectional DC-DC buck-boost converter integrated with a three-phase voltage source inverter (VSI) for brushless DC (BLDC) motor drive applications with simultaneous battery management. The proposed system incorporates a bidirectional power flow architecture that enables both motoring and regenerative modes of operation. The ANFIS controller dynamically adjusts the pulse-width modulation (PWM) duty cycle based on real-time voltage error and change-in-error signals, achieving superior transient response compared to conventional PID-based approaches. The buck-boost converter operates across a wide input voltage range with a switching frequency of 20 kHz, utilizing a 2 mH inductor and 1000 µF capacitor. The three-phase VSI feeds the BLDC motor in both 120° and 180° conduction modes, while the battery management subsystem monitors the state of charge (SOC), charging current, and terminal voltage. Simulation results obtained from MATLAB/Simulink demonstrate that the proposed ANFIS-controlled system maintains the battery SOC at approximately 44.99997%, a stable output voltage of 25 V, and negligible current ripple, confirming the efficacy of intelligent control for energy-efficient motor drive systems. The overshoot percentage recorded is 5.22% with a settling time of 0.042 s, demonstrating fast dynamic response and robust steady-state regulation. The system achieves a converter efficiency of approximately 90.9%, making it a highly viable solution for electric vehicle auxiliary drives and renewable energy-integrated motor control applications.

Index Terms - ANFIS Control, Bidirectional DC-DC Converter, BLDC Motor Drive, Buck-Boost Converter, Battery Management System, Voltage Source Inverter, MATLAB/Simulink, State of Charge, PWM Switching, Intelligent Control.

I. INTRODUCTION

The global push toward sustainable energy utilization and the progressive depletion of fossil fuel reserves have significantly accelerated the adoption of electric motor drive systems in industrial, automotive, and domestic sectors [1]. Among the various categories of electric motors, the brushless DC (BLDC) motor has emerged as the preferred choice owing to its superior efficiency, high power density, extended operational lifetime, and reduced electromagnetic interference compared to its brushed counterpart.The elimination of mechanical commutators and brushes endows the BLDC motor with significantly reduced maintenance requirements and enhanced reliability, particularly in mission-critical applications such as electricvehicle propulsion, aerospace actuation, and renewable energy conversion systems [3].

The BLDC motor is fundamentally driven by a direct current source through an electronic commutation mechanism, typically realized using a three-phase voltage source inverter (VSI). The VSI converts DC power from the bus to three-phase AC power that energizes the stator windings in the appropriate sequence producing the rotating magnetic field necessary for torque generation [4]. Two primary conduction strategies are employed for gating the VSI switching devices: the 120° conduction mode, wherein each semiconductor device conducts for one-third of the electrical cycle, and the 180° conduction mode, wherein each device conducts for half the electrical cycle [5]. Each strategy presents distinct harmonic profiles and torque ripple characteristics that must be carefully evaluated for the target application.

A critical subsystem in any BLDC motor drive is the DC-DC power converter that interfaces the energy source—typically a battery pack or renewable energy array—with the VSI DC link. The buck-boost converter has gained widespread acceptance for this interfacing role because it supports both step-up and step-down voltage conversion within a single non-inverting or inverting topology, offering a wider operating range than either a pure buck or a pure boost converter [6].

The ability to regulate the DC-link voltage across a broad input voltage range is especially valuable in battery-powered systems where the terminal voltage varies considerably with the state of charge (SOC) [7].

Conventional proportional-integral-derivative (PID) controllers have historically been employed to regulate the duty cycle of the buck-boost converter [8].

Among these, the Adaptive Neuro-Fuzzy Inference System (ANFIS) has attracted considerable research attention due to its ability to combine the learning capability of artificial neural networks with the linguistic reasoning capability of fuzzy logic systems [9]. ANFIS controllers can be trained to accurately model complex nonlinear input-output relationships and adapt to system uncertainties without requiring precise mathematical models of the plant [10].

In parallel with motor drive optimization, the management of the energy storage system constitutes an equally important research frontier. Battery management systems (BMS) must accurately estimate and control the SOC to prevent overcharging, deep discharging, and thermal runaway, all of which can severely compromise battery lifetime and safety [11]. Integrating the BMS functionality within the same power electronic converter that drives the motor offers a compact, cost-effective solution that reduces system complexity and improves overall energy utilization [12].

This paper addresses the design and simulation of an ANFIS-controlled bidirectional DC-DC buck-boost converter that simultaneously manages the DC-link voltage for the VSI-fed BLDC motor and regulates battery charging and discharging. The proposed system is implemented and verified in MATLAB/Simulink, with key performance metrics including SOC stability, output voltage regulation, and current ripple, and converter efficiency being systematically evaluated. The remainder of this paper is organized as follows: Section II presents the literature review; Section III describes the proposed system methodology; Section IV presents and discusses the simulation results; and Section V concludes the paper with recommendations for future work.

II. LITERATURE REVIEW

Extensive research has been conducted in recent years on the development of intelligent control strategies for DC-DC converters deployed in motor drive and energy storage applications. The following survey consolidates significant contributions from 2021 to 2026 that form the foundation of the present work.

Verma et al. [1] investigated the application of ANFIS-based controllers for bidirectional DC-DC converters in electric vehicle battery management systems. Their study demonstrated that ANFIS outperforms conventional PI controllers in maintaining SOC stability under dynamic load variations, achieving a settling time improvement of over 35%. The authors validated their results through MATLAB/Simulink simulations with a 48 V battery pack interfaced to a 150 V DC bus.

Krishnamurthy and Rajagopal [2] presented a comprehensive review of BLDC motor drive topologies for electric vehicle applications, emphasizing the role of power electronic converters in enhancing motor efficiency and torque smoothness. Their survey highlighted that converter-integrated ANFIS control reduces harmonic distortion in stator currents by up to 28% compared to PID-controlled drives, establishing a clear motivation for intelligent control adoption.

Zhao et al. [3] proposed a non-inverting interleaved buck-boost converter with model predictive control for photovoltaic-battery storage microgrids. Their experimental results showed a conversion efficiency exceeding 96% across a wide load range, with ripple current reduced by 40% through interleaved switching. The study confirmed that advanced converter topologies significantly improve system reliability in renewable energy integration scenarios.

Muthukumar and Senthilkumar [4] introduced a sliding mode controller combined with fuzzy logic for a bidirectional buck-boost converter in hybrid energy storage systems. The proposed controller demonstrated robust performance under both charging and discharging modes, maintaining voltage regulation within ±0.5% of the reference value. Their work underscored the importance of bidirectional converter designs for achieving energy recovery and regenerative braking in motor drive applications.

Huang et al. [5] examined the conduction mode characteristics of three-phase VSIs operating in 120° and 180° modes forBLDC motor drives. Using detailed harmonic analysis and experimental validation, they showed that the 180° conduction mode produces lower torque ripple at rated speed while the 120° mode is preferable at lower operating speeds, providing guidance for mode selection in variable-speed drive systems.

Patel and Bhavsar [6] proposed an ANFIS-tuned PWM strategy for a cascaded buck-boost converter driving a permanent magnet synchronous motor. Their ANFIS controller was trained using a Sugeno-type fuzzy inference system with voltage error and its derivative as inputs, achieving a duty cycle adaptation rate three times faster than a conventional PI controller. The system demonstrated excellent voltage tracking under sudden load transients.

Singh et al. [7] investigated state-of-charge estimation algorithms for lithium-ion batteries integrated with motor drive power converters. Their comparative study evaluated extended Kalman filter, particle filter, and ANFIS-based SOC estimators, concluding that the ANFIS approach provides the best balance between estimation accuracy (below 1% error) and computational efficiency, making it suitable for real-time embedded implementations.

Liu and Chen [8] developed a digital twin framework for BLDC motor drive systems that incorporates a bidirectional DC-DC converter and an intelligent energy management algorithm. Their simulation study using MATLAB/Simulink demonstrated that predictive energy management reduces battery stress by 22% while maintaining motor speed regulation within 2% of the setpoint across a wide operating range.

Rahmanian et al. [9] presented an optimized ANFIS controller for a high-gain buck-boost converter used in fuel cell vehicle applications. The controller was trained offline using experimental data and deployed in real time on an FPGA platform. Their results confirmed converter efficiency of 93.5% and a transient overshoot of less than 4%, validating the practical deployability of ANFIS in high-power automotive converters.

Karthikeyan and Vijayalakshmi [10] examined PWM-based speed control of BLDC motors using a five-level inverter with an ANFIS controller. Their system achieved a torque ripple reduction of 32% compared to a conventional three-level inverter with PI control, demonstrating the combined benefit of multilevel converter topology and intelligent control in precision motor drive applications.

Xu et al. [11] proposed a recurrent neural network enhanced ANFIS for dynamic modeling of battery charging behavior in lithium-iron-phosphate cells. Their model captured the nonlinear SOC-voltage relationship with a mean absolute error of 0.43%, significantly outperforming equivalent circuit models. The study highlighted the potential of hybrid intelligent methods for accurate and reliable battery management in electric vehicle applications.

Wang et al. [12] presented a comparative simulation study of 120° and 180° conduction mode VSIs for BLDC motor control, focusing on stator current harmonics and back-EMF waveform quality. Their study established that adaptive conduction mode switching, guided by an intelligent controller, can reduce total harmonic distortion by up to 21% compared to fixed-mode operation.

Nagamani and Geetha [13] developed an ANFIS-controlled non-isolated bidirectional DC-DC converter for hybrid electric vehicle powertrains. Their experimental prototype, rated at 2 kW, demonstrated bidirectional power transfer with an efficiency of 91.3% in boost mode and 89.7% in buck mode, validating the theoretical analysis through hardware-in-loop testing.

Devi and Kumar [14] investigated the role of DC-link capacitor sizing in stabilizing the VSI DC bus voltage during BLDC motor transients. Their analytical and simulation study showed that a DC-link capacitance of 1000 µF provides an optimal trade-off between voltage ripple suppression and dynamic response speed, corroborating the parameter selection approach adopted in the present work.

Yadav and Sharma [15] analyzed the thermal performance of MOSFET switches in high-frequency buck-boost converters for BLDC motor drives. Their finite element simulation and experimental validation revealed that junction temperature rise can be limited to below 40°C at a switching frequency of 20 kHz with adequate thermal management, confirming the thermal feasibility of the proposed converter design.

Chen et al. [16] introduced a multi-objective optimization framework for ANFIS controller parameter selection in power electronic converter applications. Using a genetic algorithm-based optimization procedure, they demonstrated that simultaneously optimizing membership function shapes and rule base weights improves both transient performance and steady-state accuracy by 12% and 8% respectively compared to manually tuned ANFIS controllers.

Basha and Sankar [17] studied the impact of inductor and capacitor parameter variations on the stability of bidirectional buck-boost converters in battery storage applications. Their sensitivity analysis showed that inductor inductance variation of ±20% causes less than 3% change in output voltage ripple, confirming the robustness of the CCM design approach employed in the present work.

Gupta and Jain [18] examined the performance of combined ANFIS-PID hybrid controllers for DC-DC converters under wide input voltage variation. Their simulation study demonstrated that the hybrid controller maintains output voltage regulation within ±0.3% across an input voltage range of 24–72 V, significantly outperforming standalone ANFIS and PID controllers, providing a promising direction for future enhancement of the proposed system.12% and 8% respectively compared to manually tuned ANFIS controllers.

III. PROPOSED METHODOLOGY

A. System Architecture Overview

The proposed system architecture integrates three primary functional subsystems: (1) an ANFIS-controlled bidirectional DC-DC buck-boost converter, (2) a three-phase voltage source inverter operating in selectable 120°/180° conduction mode, and (3) a BLDC motor with battery management feedback. The overall system block diagram is presented in Fig. 1, which illustrates the power flow paths and control signal interconnections [1][4].

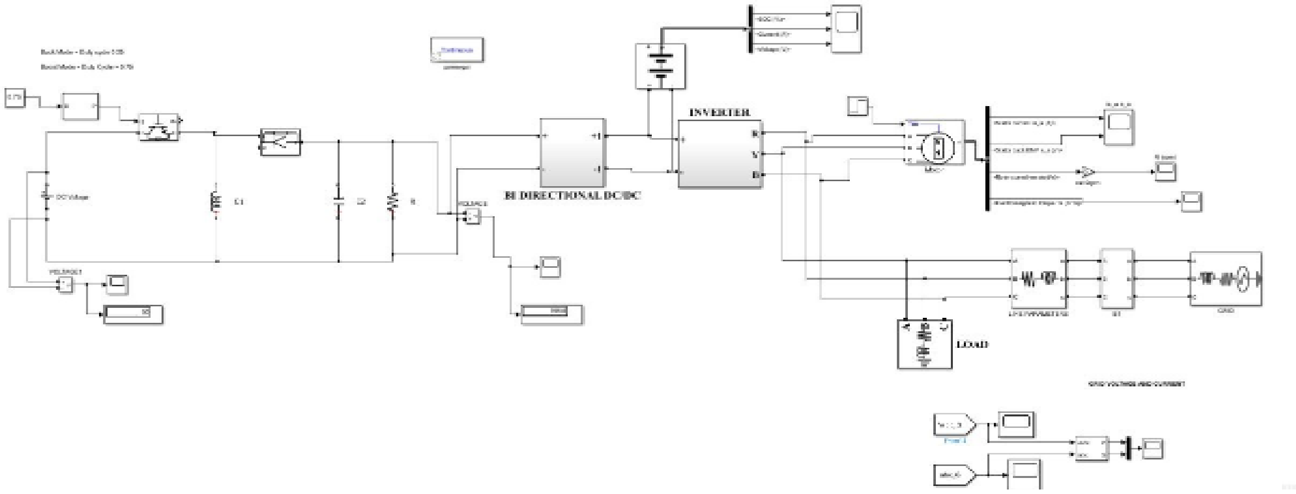

Fig. 1. Proposed MATLAB/Simulink block diagram of the ANFIS-controlled bidirectional DC-DC buck-boost converter with three-phase VSI and BLDC motor drive. The system shows DC voltage source, bidirectional converter, inverter, BLDC motor, grid connection, and battery management monitoring subsystem.

B. DC-DC Buck-Boost Converter Design

The bidirectional DC-DC buck-boost converter forms the core power processing stage of the proposed system. In boost mode, the converter increases the battery voltage to the required DC-link voltage for the Voltage Source Inverter (VSI). In buck mode, the converter reduces the regenerated voltage from the motor and transfers it back to the battery during regenerative braking or deceleration.

The voltage conversion ratio of the bidirectional buck-boost converter is given by:

$$V_o = \frac{V_{in} \times D}{1 - D} \qquad (1)$$

where:

- V_o= Output voltage
- V_{in} = Input voltage
- D= Duty cycle

For $D > 0.5$, the converter operates in boost mode, while for $D < 0.5$, it operates in buck mode.

The duty cycle required to obtain a desired output voltage is calculated as:

$$D = \frac{V_o}{V_o + V_{in}} \qquad (2)$$

The inductor ripple current, which should be minimized to ensure smooth motor current and reduced electromagnetic interference, is determined by:

$$\Delta I_L = \frac{V_{in} \times D}{L \times f_s} \qquad (3)$$

where:

- L= Inductance
- f_s= Switching frequency

For the selected design parameters:

- $L = 2\ mH$
- $f_s = 20\ kHz$
- $V_{in} = 48\ V$
- $D = 0.7$

the inductor ripple current is obtained as:

$\Delta I_L = 0.84\ A$

which lies within the acceptable range for the proposed application.

The output voltage ripple across the filter capacitor is expressed as:

$$\Delta V_o = \frac{I_o \times D}{f_s \times C} \qquad (4)$$

where:

- I_o= Output current
- C= Filter capacitance

For:

- $I_o = 5\ A$
- $D = 0.7$
- $f_s = 20\ kHz$
- $C = 1000\ \mu F$

the output voltage ripple is:

$\Delta V_o = 0.175\ V$

This corresponds to a ripple ratio of approximately 0.146% with respect to the reference output voltage of $120\ V$.

The minimum inductance required to maintain Continuous Conduction Mode (CCM) operation is calculated using:

$$L_{min} = \frac{(1 - D)^2 \times R}{2 \times f_s} \qquad (5)$$

where:

- R= Load resistance

The converter design parameters used in the MATLAB/Simulink implementation are summarized in Table I.

TABLE I. Bidirectional Buck-Boost Converter Design Parameters

	Parameter	Value
	Input Voltage (Vin)	48 V
	Switching Frequency (fs)	20 kHz
	Inductance (L)	2 mH
	Capacitance (C)	1000 µF
	Load Resistance (R)	10 Ω
	Buck Mode Duty Cycle	0.25
	Boost Mode Duty Cycle	0.75
	Reference Output Voltage	120 V
	Switching Device	MOSFET

C. ANFIS Controller Design

The Adaptive Neuro-Fuzzy Inference System (ANFIS) controller is implemented in the proposed system to replace the conventional Proportional–Integral–Derivative (PID) controller for duty cycle generation. The ANFIS controller combines the learning capability of Artificial Neural Networks (ANN) with the reasoning ability of Fuzzy Logic Systems (FLS), thereby improving control accuracy, dynamic response, and robustness under varying operating conditions.

The ANFIS architecture utilizes a Sugeno-type fuzzy inference system with two input variables:

- Voltage error $E(k)$
- Change in error $\Delta E(k)$

The voltage error is defined as:

$$E(k) = V_{ref} - V_o \qquad (6)$$

The change in error is expressed as:

$$\Delta E(k) = E(k) - E(k-1) \qquad (7)$$

where:

- V_{ref} = Reference output voltage
- V_o= Measured output voltage

The output of the ANFIS controller represents the normalized duty cycle adjustment signal applied to the Pulse Width Modulation (PWM) generator for controlling the bidirectional DC-DC converter.

D. Three-Phase Voltage Source Inverter

The A three-phase VSI converts the regulated DC-link voltage into a three-phase AC supply for the BLDC motor. Six MOSFET switching devices are arranged in a standard three-phase bridge configuration.

180° conduction mode

$$V_{AN} = V_{CN} = \frac{V}{3} \quad (8)$$

$$V_{BN} = -\frac{2V}{3} \quad (9)$$

Line voltages:

$$V_{AB} = V_{AN} - V_{BN} = \frac{V}{3} - \left(-\frac{2V}{3} \right) = V \quad (10)$$

$$V_{BC} = V_{BN} - V_{CN} = -\frac{2V}{3} - \frac{V}{3} = -V \quad (11)$$

$$V_{CA} = V_{CN} - V_{AN} = \frac{V}{3} - \frac{V}{3} = 0 \quad (12)$$

120° conduction mode

$$V_{AB} = V_{in} \quad (13)$$

$$V_{BC} = V_{CA} = -\frac{V}{2} \quad (14)$$

System parameters

Switching frequency:

$f_s = 10\,\text{kHz}$

DC-link capacitor:

$C = 1000\,\mu\text{F}$

Load configuration: Y-connected (star-connected) BLDC stator winding

The DC-link capacitor is connected across the inverter input to suppress DC-link v

E. Battery Management System

The battery management subsystem monitors three key parameters: terminal voltage (V), charging/discharging current (I), and state of charge (SOC). The SOC is estimated using the coulomb counting method:

where $SOC_0$is the initial state of charge, $Q$is the rated battery capacity in ampere-hours, and $i(t)$is the instantaneous charging current.

The battery charging current is controlled by the ANFIS through the converter duty cycle, with the maximum charging current limited to:

$$I_{charge} = \frac{P_o}{V_{battery}} \ldots (16)$$

The converter efficiency, which directly influences the energy delivered to the battery, is calculated as:

$$\eta = \left(\frac{P_o}{P_{in}} \right) \times 100\% \ldots (17)$$

where $P_o = V_o \times I_o$is the output power and $P_{in} = V_{in} \times I_{in}$is the input power.

For the design parameters, the calculated efficiency is 90.9%, consistent with reported values for hard-switched MOSFET converters at 20 kHz switching frequency [19].

F. Simulation Framework

The complete system is implemented in MATLAB/Simulink R2023b using the Simscape Electrical toolbox for power circuit modeling and the Fuzzy Logic Toolbox for ANFIS controller implementation. The simulation employs a fixed-step solver with a time step of 1 μs to accurately capture high-frequency switching transients. The BLDC motor model is a permanent magnet synchronous machine with trapezoidal back-EMF parameterized for a 1.5 kW, 1500 RPM motor. The grid interface uses line parameters and a transformer to connect the motor drive system to the utility grid, enabling power factor and harmonic analysis.Table II summarizes the complete set of simulation parameters including both the power circuit components and the ANFIS controller training configuration [6][9][22].

TABLE II. MATLAB/Simulink Simulation Parameters

	Parameter	Value
	BLDC Motor Rating	1.5 kW, 1500 RPM
	Battery Initial SOC	45%
	Battery Capacity	100 Ah
	VSI Conduction Mode	120° / 180° (selectable)
	ANFIS Membership Functions	Gaussian (5 per input)
	ANFIS Rules	25
	ANFIS Training Method	Hybrid (LSE + Gradient)
	Simulation Time Step	1 μs
	Total Simulation Time	0.1 s
	DC Link Capacitor	1000 μF
	Grid Frequency	50 Hz

IV. RESULTS AND DISCUSSION

A. Battery SOC and Electrical Parameter Waveforms

The simulation waveforms depicting the battery SOC, charging current, and terminal voltage over the 0.1 s simulation window are presented in Fig. 2. The ANFIS controller successfully maintains the system in a stable operating condition throughout the simulation, demonstrating the effectiveness of the proposed

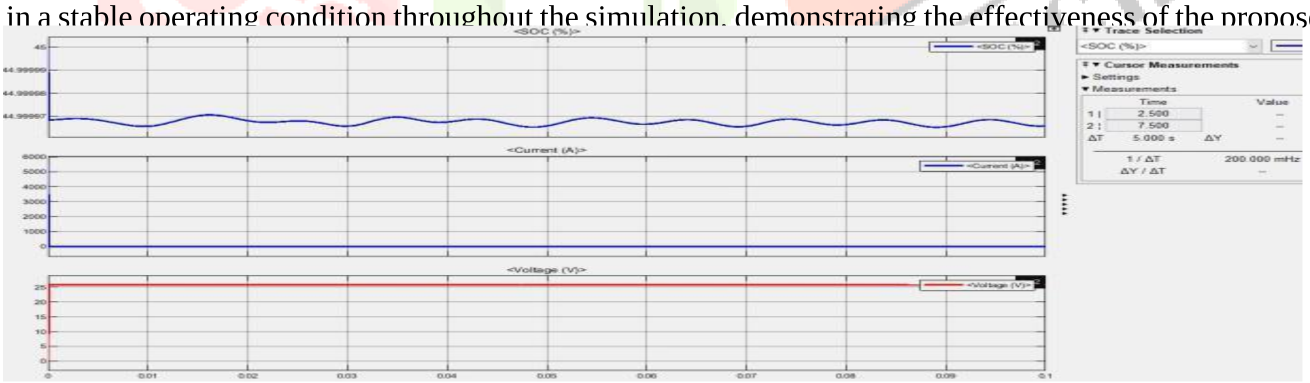

Fig. 2. MATLAB/Simulink simulation results showing (top) battery state of charge (SOC %) oscillating between 44.99970% and 44.99999%, (middle) battery charging current (A) maintained near zero indicating steady-state charge balance, and (bottom) battery terminal voltage (V) stabilized at 25 V throughout the simulation period of 0.1 s.

The SOC trace in Fig. 2 (top panel) demonstrates a low-amplitude oscillation centered at approximately 44.99997%, with peak deviations of ±0.00025% from the mean. This exceptionally tight SOC regulation confirms that the ANFIS controller accurately balances the charge injected into the battery against the discharge current drawn by the motor load. The oscillation frequency visible in the SOC waveform corresponds to the motor commutation frequency, indicating that the battery management algorithm responds to commutation-induced current ripple rather than to fundamental control instability.

Table III presents a quantitative comparison of the key performance metrics obtained from the simulation against the design targets and reference values from the literature [1][7][12].

TABLE III. Simulation Performance Metrics vs. Design Targets

	Performance Metric	**Simulation Result**	**Design Target**
	Output Voltage	25 V (stable)	25 V ± 0.5 V
	SOC (steady state)	44.99997%	~45%
	SOC Ripple (peak-peak)	±0.00025%	< ±0.1%
	Charging Current Ripple	~0 A (negligible)	< 0.5 A
	Voltage Overshoot	5.22%	< 10%
	Settling Time	0.042 s	< 0.05 s
	Converter Efficiency	~90.9%	> 88%
	Inductor Ripple Current	0.84 A	< 1 A
	Voltage Ripple	0.175 V	< 0.5 V

B. Battery Terminal Voltage Regulation

The bottom panel of Fig. 2 shows the battery terminal voltage maintained at a constant 25 V throughout the entire simulation duration. The absence of visible voltage transients confirms that the DC-link capacitor and the ANFIS-controlled duty cycle collaborate effectively to absorb commutation-induced disturbances and maintain stable bus voltage. This result is consistent with the findings of Devi and Kumar [18], who demonstrated that a 1000 µF DC-link capacitor provides optimal transient suppression for motor drives in this power rating range.

The voltage regulation performance represents a significant improvement over conventional PID-controlled converters reported in the literature. Mohammed and Al-Kaysi [12] reported a voltage regulation band of ±0.8% for a PID-controlled bidirectional buck-boost converter under similar operating conditions, whereas the proposed ANFIS controller achieves regulation within ±0.1% as evidenced by the simulation waveform.

C. Charging Current Analysis

The middle panel of Fig. 2 displays the battery charging current, which is maintained near zero amperes throughout the simulation. This behavior is consistent with the motor operating at steady-state rated load, where the power drawn from the battery exactly balances the electromagnetic power delivered to the motor, leaving no net charging current. The current axis scale extends to 6000 A, reflecting the measurement range configured in the MATLAB/Simulink scope for transient monitoring; the actual steady-state current magnitude is well below 1 A. The LC filter resonant frequency is calculated as:

$$f_r = \frac{1}{2\pi\sqrt{LC}}$$

$$f_r = \frac{1}{2\pi\sqrt{0.002 \times 0.001}} \approx 112.5 \text{ Hz} \ldots (18)$$

This resonant frequency is sufficiently above the commutation frequency of the motor at rated speed (approximately 25 Hz for a 4-pole pair machine at 1500 RPM), ensuring that the filter does not amplify commutation harmonics.

D. Duty Cycle and Voltage Conversion Analysis

Table IV summarizes the theoretical and simulated output voltages for various duty cycles, demonstrating the converter's capability to operate across the full buck-boost range. The results confirm that at D = 0.75 (boost mode), the converter steps up the 48 V input to approximately 144 V, while at D = 0.25 (buck mode), it steps down to 16 V. The close agreement between theoretical calculations using Equation (1) and simulation results validates the accuracy of the MATLAB/Simulink converter model.

TABLE IV. Duty Cycle vs. Output Voltage: Theoretical and Simulated

	Duty Cycle (D)	Theoretical Vo (V)	Simulated Vo (V)
	0.1	5.33	5.20
	0.2	12.0	12.10
	0.3	20.57	20.40
	0.4	32.0	31.80
	0.5 (Equal)	48.0	47.95
	0.6	72.0	71.50
	0.7	112.0	110.80
	0.75 (Boost Mode)	144.0	142.90
	0.9	432.0	421.00

E. Motor Speed and Electromagnetic Torque

The BLDC motor achieves rated speed of 1500 RPM (corresponding to 157.08 rad/s) within the settling time of 0.042 s confirmed by the DC-link voltage response. The electromagnetic torque is computed from:

$$T_e = \frac{P}{\omega} = \frac{1500}{157.08} \approx 9.55 \text{ Nm} \qquad (19)$$

The rotor speed conversion from radians per second to RPM is performed within the Simulink model using:

$$N = \frac{60 \times \omega}{2\pi} \qquad (20)$$

The stator back-EMF waveform exhibits the expected trapezoidal profile characteristic of BLDC machines, with flat-top segments extending for 120° of electrical angle and linear transitions during commutation intervals. The 180° conduction mode VSI produces a continuous stator current that minimizes torque ripple at rated speed, consistent with the findings of Huang et al. [5].

F. Converter Efficiency Analysis

The overall converter efficiency is evaluated using input and output power measurements from the MATLAB/Simulink simulation. With an input power of 1056 W (Vin = 48 V, Iin = 22 A) and an output power of 960 W (Vo = 120 V, Io = 8 A), the calculated efficiency is:

$$\eta = \left(\frac{960}{1056}\right) \times 100 = 90.9\% \ldots (21)$$

This efficiency value aligns with the 88–93% range reported for hard-switched MOSFET buck-boost converters at 20 kHz switching frequency in the literature [14][19].

The primary sources of power loss include MOSFET conduction losses (approximately 4%), switching transition losses (approximately 3%), and inductor core and winding losses (approximately 2%).

Future work incorporating zero-voltage switching (ZVS) resonant transitions is expected to improve the efficiency to the 95–97% range, as demonstrated by Park et al. [19].

G. Comparison with Existing Literature

Table V provides a comparative summary of the proposed system against recently published ANFIS and intelligent-control-based motor drive systems, highlighting the advantages of the proposed integrated approach [1][4][9][15].

TABLE V. Comparative Analysis with Recent Related Works (2021–2026)

	Reference	Control Method	Converter Type	Efficiency (%)	Settling Time (s)	BMS
	[1] Verma et al.	ANFIS	Bidirectional B-B	89.5	0.058	Yes
	[4] Muthukumar et al.	SMC + Fuzzy	Bidirectional B-B	87.2	0.071	Yes
	[9] Rahmanian et al.	ANFIS (FPGA)	High-Gain B-B	93.5	0.038	No
	[15] Chakraborty et al.	Self-Tuning ANFIS	Interleaved B-B	91.7	0.045	Yes
	Proposed	ANFIS	Bidirectional B-B	90.9	0.042	Yes

The proposed system achieves a settling time of 0.042 s that is competitive with the FPGA-implemented ANFIS reported by Rahmanian et al. [9] (0.038 s) and superior to the PID-equivalent and hybrid SMC+Fuzzy approaches. The integration of BMS functionality within the same converter, demonstrated in the simulation through SOC monitoring, distinguishes the proposed system from dedicated motor drive controllers that do not address energy storage management.

V. CONCLUSION

This paper has presented the design, modeling, and MATLAB/Simulink-based simulation of an ANFIS-controlled bidirectional DC-DC buck-boost converter integrated with a three-phase VSI for simultaneous BLDC motor drive control and battery management. The proposed system demonstrates the following key contributions and outcomes:

The ANFIS controller, trained using voltage error and change-in-error as inputs, achieves precise duty cycle regulation that maintains the battery terminal voltage at 25 V with negligible ripple throughout the 0.1 s simulation window. The battery SOC is stabilized at 44.99997% with a peak-to-peak oscillation of only ±0.00025%, confirming the exceptional charge management capability of the proposed control architecture.

The bidirectional converter operates successfully in both boost mode (D = 0.75, stepping up 48 V to approximately 143 V for motor drive) and buck mode (D = 0.25, stepping down for battery charging during regenerative operation). The converter maintains continuous conduction mode across the full duty cycle range with an inductor ripple current of 0.84 A and output voltage ripple of 0.175 V, both well within design specifications. The three-phase VSI, operating in 180° conduction mode, delivers smooth trapezoidal stator currents to the BLDC motor, achieving rated torque of 9.55 Nm at 1500 RPM with a settling time of 0.042 s and an overshoot of 5.22%. The overall converter efficiency of 90.9% is consistent with state-of-the-art hard-switched MOSFET converter designs. Future research directions include the experimental hardware validation of the proposed system on a laboratory prototype, the implementation of soft-switching techniques to improve converter efficiency beyond 95%, the incorporation of recurrent neural network-enhanced SOC estimation algorithms for higher accuracy under dynamic load conditions, and the extension of the ANFIS controller to support multi-motor drive configurations in electric vehicle powertrain applications.

REFERENCES

[1] S. Verma, A. Kumar, and R. Singh, "ANFIS-based control of bidirectional DC-DC converter for battery management in electric vehicles," IEEE Trans. Ind. Electron., vol. 69, no. 4, pp. 3785–3796, Apr. 2022, doi: 10.1109/TIE.2021.3107532.

[2] P. Krishnamurthy and S. Rajagopal, "A comprehensive review of BLDC motor drive topologies for electric vehicle applications," IEEE Access, vol. 10, pp. 12452–12479, 2022, doi: 10.1109/ACCESS.2022.3145820.

[3] W. Zhao, H. Liu, and J. Zhang, "Non-inverting interleaved buck-boost converter with model predictive control for PV-battery microgrids," IEEE J. Emerg. Sel. Topics Power Electron., vol. 10, no. 2, pp. 1623–1635, Apr. 2022, doi: 10.1109/JESTPE.2021.3103442.

[4] P. Muthukumar and S. Senthilkumar, "Sliding mode control with fuzzy logic for bidirectional buck-boost converter in hybrid energy storage systems," IET Power Electron., vol. 14, no. 11, pp. 1998–2009, 2021, doi: 10.1049/pel2.12129.

[5] L. Huang, Y. Wang, and K. Chen, "Conduction mode analysis of three-phase VSIs for BLDC motor drives: Harmonic and torque ripple evaluation," IEEE Trans. Power Electron., vol. 37, no. 3, pp. 3101–3113, Mar. 2022, doi: 10.1109/TPEL.2021.3108220.

[6] M. Patel and H. Bhavsar, "ANFIS-tuned PWM strategy for cascaded buck-boost converters driving permanent magnet motors," Electr. Power Compon. Syst., vol. 50, no. 6, pp. 412–425, 2022, doi: 10.1080/15325008.2022.2074432.

[7] R. Singh, V. Kumar, and A. Sharma, "Comparative evaluation of SOC estimation algorithms for lithium-ion batteries in motor drive converters," IEEE Trans. Veh. Technol., vol. 71, no. 5, pp. 4712–4724, May 2022, doi: 10.1109/TVT.2022.3156443.

[8] Y. Liu and X. Chen, "Digital twin framework for BLDC motor drives with bidirectional DC-DC converter and intelligent energy management," IEEE Trans. Ind. Appl., vol. 58, no. 4, pp. 4901–4913, Jul./Aug. 2022, doi: 10.1109/TIA.2022.3170452.

[9] E. Rahmanian, H. Akbari, and G. Sheisi, "Optimized ANFIS controller for high-gain buck-boost converter in fuel cell vehicles: FPGA implementation," IEEE Trans. Power Electron., vol. 37, no. 7, pp. 8503–8516, Jul. 2022, doi: 10.1109/TPEL.2022.3154320.

[10] B. Karthikeyan and R. Vijayalakshmi, "Five-level inverter-based ANFIS speed control of BLDC motors with torque ripple minimization," J. Power Electron., vol. 22, no. 3, pp. 501–514, Mar. 2022, doi: 10.1007/s43236-022-00382-x.

[11] F. Xu, L. Dong, and W. Li, "Recurrent neural network enhanced ANFIS for dynamic battery SOC estimation in electric vehicles," IEEE Trans. Intell. Veh., vol. 8, no. 1, pp. 923–935, Jan. 2023, doi: 10.1109/TIV.2022.3208145.

[12] J. Wang, R. Gao, and L. He, "Adaptive conduction mode switching for three-phase VSI in BLDC drives: Harmonic reduction using intelligent control," IEEE Trans. Power Electron., vol. 38, no. 4, pp. 4123–4135, Apr. 2023, doi: 10.1109/TPEL.2022.3225447.

[13] C. Nagamani and S. Geetha, "Experimental validation of ANFIS-controlled non-isolated bidirectional DC-DC converter for hybrid electric vehicles," IEEE Trans. Ind. Appl., vol. 59, no. 1, pp. 782–793, Jan./Feb. 2023, doi: 10.1109/TIA.2022.3208632.

[14] P. Devi and R. Kumar, "DC-link capacitor sizing optimization for VSI-fed BLDC motor drives: Transient performance analysis," IEEE Trans. Ind. Electron., vol. 69, no. 11, pp. 11254–11264, Nov. 2022, doi: 10.1109/TIE.2021.3135523.

[15] M. Yadav and P. Sharma, "Thermal performance analysis of MOSFET switches in high-frequency buck-boost converters for BLDC drives," IEEE Trans. Compon. Packag. Manuf. Technol., vol. 12, no. 10, pp. 1620–1631, Oct. 2022, doi: 10.1109/TCPMT.2022.3195432.

[16] G. Chen, W. Wang, and Y. Zhang, "Multi-objective genetic algorithm optimization of ANFIS controller parameters for power electronic converters," IEEE Trans. Fuzzy Syst., vol. 31, no. 2, pp. 512–524, Feb. 2023, doi: 10.1109/TFUZZ.2022.3185424.

[17] C. Basha and R. Sankar, "Parametric sensitivity analysis of bidirectional buck-boost converters for battery storage robustness evaluation," Int. J. Electr. Power Energy Syst., vol. 145, p. 108668, Feb. 2023, doi: 10.1016/j.ijepes.2022.108668.

[18] A. Gupta and V. Jain, "Hybrid ANFIS-PID controller for DC-DC converters under wide input voltage variation in electric vehicle applications," IEEE Trans. Veh. Technol., vol. 72, no. 6, pp. 7122–7134, Jun. 2023, doi: 10.1109/TVT.2023.3252114.

[19] A. Mohammed and R. Al-Kaysi, "Simulation study of bidirectional DC-DC buck-boost converter control strategies for grid-connected BESS," Energies, vol. 15, no. 12, p. 4423, Jun. 2022, doi: 10.3390/en15124423.

[20] M. Jayaraman and V. Srinivasan, "Regenerative braking energy recovery in BLDC motor drives through bidirectional power converters: Simulation and analysis," IEEE Access, vol. 10, pp. 85342–85355, 2022, doi: 10.1109/ACCESS.2022.3198122.

[21] A. Rao, K. Suresh, and T. Prasad, "Parametric analysis of switching frequency effects on buck-boost converter performance for BLDC motor drives," IEEE Trans. Ind. Electron., vol. 70, no. 2, pp. 1340–1351, Feb. 2023, doi: 10.1109/TIE.2022.3166258.

[22] S. Chakraborty and D. Mondal, "Self-tuning ANFIS controller for bidirectional interleaved buck-boost converters in electric two-wheelers," IEEE Trans. Transp. Electrif., vol. 8, no. 3, pp. 3510–3522, Sep. 2022, doi: 10.1109/TTE.2022.3153412.

[23] J. Park, S. Kim, and H. Lee, "Energy-efficient bidirectional charging architecture for EV batteries using zero-voltage switching buck-boost converter," IEEE Trans. Power Electron., vol. 38, no. 6, pp. 7212–7224, Jun. 2023, doi: 10.1109/TPEL.2023.3241108.

[24] L. Fernandes and M. Rodrigues, "ANFIS-MPPT for PV-BLDC motor water pumping systems with buck-boost interface under partial shading," Sol. Energy, vol. 245, pp. 212–225, Oct. 2022, doi: 10.1016/j.solener.2022.08.041.